

**NASA TECHNICAL  
MEMORANDUM**

NASA TM X- 52940

NASA TM X- 52940

**CASE FILE  
COPY**

**PRELIMINARY RESULTS OF THE OPERATION OF A  
SERT II THRUSTER ON ARGON**

by Ronald J. Schertler  
Lewis Research Center  
Cleveland, Ohio

**TECHNICAL PAPER** proposed for presentation at  
Ninth Aerospace Sciences Meeting sponsored by the  
American Institute of Aeronautics and Astronautics  
New York, New York, January 25-27, 1971

Ronald J. Schertler  
Lewis Research Center  
National Aeronautics and Space Administration  
Cleveland, Ohio

### Abstract

Preliminary results of the operation of a SERT II type, 15-cm electron bombardment thruster are reported. Results of incorporating an enclosed keeper into the thruster cathode design show that open and enclosed keeper cathodes yield comparable performance with mercury. Initial performance data with argon indicate that both low discharge chamber losses (240 eV/ion) and high propellant utilization efficiencies (>85%) are obtainable. Discharge chamber performance with argon compares favorably with that of the SERT II mercury thruster. The discharge within the cathode-keeper region and the associated power level of keeper operation were found to influence the overall argon performance data.

### Introduction

Bombardment thruster operation using various gas propellants was reported in 1964 by Reader<sup>(1)</sup> for a 10-cm thruster with a thermionic (wire) cathode. Performance was generally limited to low propellant utilization efficiencies and high discharge chamber losses (eV/ion). Advances in thruster component technology, primarily as a result of the SERT II flight test program, allow reevaluation of thruster performance with the various gas propellants. Also, better understanding of the discharge chamber phenomena should result from correlating the thruster performance while operating with various gaseous propellants having different atomic masses, ionization potentials, and electron impact ionization cross sections. Performance correlation would be expected to improve design and scaling criteria and in predicting ion source performance.

A long-life, high efficiency ion source operating on a variety of propellants and producing a wide range of beam currents should find numerous applications such as biowaste propellant thruster, preflight testing of spacecraft systems, ion technology, and plasma discharge studies. For example, in the preflight testing of a complete electric propulsion spacecraft system, the use of mercury propellant might degrade or contaminate thermal control surface coatings, solar cell arrays or other spacecraft hardware due to propellant reflection from the facility which would not occur in space. In the area of ion technology, the application of thruster ion source technology to ion plating, implantation, and machining offers exciting possibilities. As an example of one application, the thruster also provided a plasma background for a variable bias solar cell experiment while the current series of performance tests reported herein were being conducted.

The SERT II thruster used for these tests was modified to incorporate an enclosed keeper cathode. Thruster performance results are first presented for mercury propellant with the enclosed keeper design. These mercury results serve as reference performance base for the thruster. The initial results of the operation of the 15-cm electron bom-

bardment thruster on argon are then presented.

### Apparatus and Procedure

#### Thruster

The 15-cm diameter thruster used in this investigation was a modification of the Space Electric Rocket Test II (SERT II) thruster.<sup>(2,3)</sup> A sketch of the thruster is shown in Fig. 1. The anode, discharge chamber, screen and accelerating grids, magnetic screen collar and pole piece, magnetic distributor and pole piece, and propellant feed chambers essentially followed the SERT II design. Thruster components including the cathode, keeper, magnets and neutralizer were modified from the SERT II design.

The hollow cathode consisted of a 6.4 mm diameter tantalum tube with a 0.4 mm (typical) diameter orifice located in a 1.0 mm thick, 2 percent thoriated-tungsten disc electron-beam welded to the end. The cathode tip was heated by a swaged tantalum heater. This size cathode (larger than the SERT II cathode of 3.2 mm diameter) was incorporated in anticipation of emission currents in the range of 5 to 6 amperes for gaseous propellant operation.

A major departure from the SERT II design was the incorporation of an enclosed keeper.<sup>(4)</sup> A sketch of the enclosed keeper is shown in Fig. 1(a). The tantalum keeper cap was 0.25 mm thick and had a 3.2 mm diameter aperture. The keeper was positioned between 0.75 mm and 1.5 mm from the cathode aperture by means of a ceramic tube over the cathode body.

The baffle was modified from the 2.54 cm diameter, six hole SERT II baffle, mounted slightly forward of the distributor pole piece, to that of a 2.0 cm diameter solid disk mounted flush with the end of the distributor pole piece. Previous results with mercury<sup>(5)</sup> have shown that the flush baffle position resulted in an improvement in the discharge chamber characteristics resulting in slightly lower discharge chamber losses (eV/ion) and discharge chamber voltage,  $\Delta V_1$ . No optimization of the baffle was attempted for argon propellant.

Eight electromagnets, uniformly located around the discharge chamber, provided a variable strength magnetic field. A divergent magnetic field shape was produced by two magnetic pole pieces and the magnetic screen collar. This divergent field shape was similar to that of the SERT II thruster. The axial magnetic field strength, measured a few millimeters downstream of the baffle, was  $4 \times 10^{-3}$  W/m<sup>2</sup>. The corresponding value for the SERT II thruster was  $3.2 \times 10^{-3}$  W/m<sup>2</sup>. Preliminary performance results with mercury indicated that for the divergent magnetic field the discharge chamber losses were minimized for an axial magnetic field strength of  $4 \times 10^{-3}$  W/m<sup>2</sup> over the complete range of neutral flow rates and beam currents used. All data presented

herein was obtained with this axial magnetic field strength.

The molybdenum screen and accelerator grids were the same type used in the SERT II thruster. The open area of the screen and accelerator grids were 72 and 50 percent, respectively. Grid spacing was about 2.3 mm. The net extraction voltage was 3000 volts while the accelerator voltage was -2000 volts for the mercury runs. These values provided good discharge chamber performance with accelerator drain currents less than one percent of the beam current.

Beam neutralization was accomplished by secondary emission from the walls of the vacuum facility. Several runs were made with a hot wire neutralizer and the results were found to be identical with tank neutralization.

#### Propellant Feed System

The most important parameters for the determination of either thruster or ion source performance is the propellant flow rate. A separate propellant feed system for the cathode and main discharge chamber was used for all tests.

**Mercury.** - The mercury propellant feed system utilized two porous tungsten vaporizers 6.3 mm in diameter. Flow measurements were determined by measuring the change in height of the mercury column in a precision bore glass tube in a given time. Particular care was taken to insure thermal equilibrium of the flow system to eliminate propellant expansion effects.

**Argon.** - An argon calibration system<sup>(7)</sup> was employed directly, rather than using valves or leaks which were previously calibrated. Figure 2 is a general schematic of the cathode mass flow calibration apparatus. This system has the advantage of allowing the measurement of low flow rates over a wide range of pressure (50 to 760 torr) and also of allowing flow measurements to be made during a test while other thruster parameters were being measured. For thruster operation, two separate flow calibration systems were used; one for the cathode flow,  $J_{ok}$ , the other for the flow to the main discharge chamber,  $J_{om}$ .

Basically, the system consists of a volumetric calibrator which has been modified for operation below atmospheric pressure. The major components of the system include the propellant gas supply, flow calibrator tube, supply and accumulator tanks, and a thruster flow control valve. A pressure regulator capable of operating between 5 and 650 torr was also incorporated in the system. Flow rates were controlled with the pressure,  $P_1$ , and the thruster flow control valve. The flow measurement procedure consisted of trapping a volume of propellant gas between a liquid mercury sealed piston and the thruster at the desired pressure. The mass flow rate can be determined from the rate of change in the displacement of the piston along with the pressure and temperature downstream of the piston by:

$$\dot{m} = \rho \cdot \frac{V_d}{\Delta t} = \frac{P_1 V_d}{R_0 T_1 \Delta t}$$

where

$\rho$	gas density downstream of piston
$V_d$	volume displacement
$\Delta t$	time lapse for displacement
$P_1$	pressure downstream of piston
$R_0$	gas constant
$T_1$	temperature downstream of piston

One possible source of error within the system is the change in system pressure over one calibration run. Both the supply tank (30 liter) and the accumulator tank (15 liter) were of sufficiently large volume compared to the volume displacement of a calibration run (approximately 0.2 liter) that the maximum change in pressure over a calibration run was approximately 1/2 percent.

#### Vacuum Facilities

**Mercury.** - All mercury tests were conducted in a 1.5 meter diameter, 4.5 meter long vacuum tank. The thruster was mounted in a metal bell jar separated from the tank by a 0.9 meter diameter gate valve. Tank pressure varied from 4 to  $8 \times 10^{-6}$  torr and bell jar pressures from  $7 \times 10^{-6}$  torr to  $1 \times 10^{-5}$  torr during thruster operation. The tank contains a liquid nitrogen cooled cryogenic liner.

**Argon.** - A separate vacuum facility, 3 meters in diameter and 5.8 meters long,<sup>(6)</sup> was used with the argon propellant tests because of the need for high pumping capacity with the non-condensable propellant. In this facility the tank pressure could be maintained in the  $10^{-6}$  torr range for neutral flow rates equivalent to one ampere. The thruster was mounted from the end cap of the facility as shown in Fig. 3. The ground screen cowling which surrounded the mounting support rods and the electrical wiring are not shown.

#### Startup Procedures

The general proceduring for starting the discharge with both mercury and argon propellants was about the same. With argon however, a higher keeper potential and a higher flow rate was required.

The cathode was heated to approximately 1100° C. A potential of 600 volts was applied to the keeper. Propellant flow was established to both the cathode and main discharge chamber. Initiation of the cathode-keeper discharge generally required a high volume of argon flow through the cathode. This high flow rate (between 5 and 10 amperes of equivalent neutral current) was provided by a bypass valve (around the thruster flow control valve) in the cathode flow system (fig. 2). This flow rate raised the pressure sufficiently in the cathode-keeper region to permit electrical breakdown at a starting voltage of 600 volts. Transfer of the cathode keeper discharge to the main anode was accomplished by applying potential to the anode.

#### Results and Discussion

##### Mercury Performance

The results of the initial phase of this pro-

gram provided a calibration of the base operating performance of the 15-cm thruster using mercury propellant and an enclosed keeper. The enclosed keeper design, first used in the 5-cm mercury bombardment thruster program,<sup>(4)</sup> reduced cathode heat losses and provided positive spacing and alignment of the keeper electrode. In a 5-cm thruster, the enclosed keeper also demonstrated greater operational stability over a wider range of discharge variables than the open (SERT II) keeper.

Figure 4 illustrates the discharge chamber performance with an enclosed keeper for various ratios of cathode to total propellant flow. The discharge chamber losses (eV/ion) as a function of propellant utilization efficiency are shown in Fig. 4(b). The total neutral flow, expressed as equivalent electrical current,  $J_0$ , was typically 0.3 amperes. The cathode neutral flow,  $J_{0k}$ , was varied between 19 and 30 percent of the total neutral flow. At the lower cathode neutral flow rates, and the lower propellant utilization efficiencies, the discharge losses are relatively high (200 to 250 eV/ion). The lower cathode flow rates however did result in the highest propellant utilization efficiencies obtainable. At the higher cathode neutral flow rates the discharge losses at the lower propellant utilization efficiencies are reasonably low (170 eV/ion) but propellant utilization efficiencies above approximately 85 percent could not be obtained.

The discharge chamber voltage,  $\Delta V_1$ , is presented in Fig. 4(a) as a function of propellant utilization efficiency for the same ratio of cathode to total propellant flow. The discharge voltage exhibits a moderate range (33 to 46 V) of variation. Results for the higher propellant utilization efficiencies follow the same general curve, at least for the fraction of cathode to total propellant flow investigated.

Figure 5 compares the discharge chamber losses between open keeper (ring type, SERT II design) and enclosed keeper configurations for mercury propellant. Results are presented for two different ratios of cathode to total propellant flow. The data were obtained under constant neutral flow conditions while the discharge chamber current and voltage was varied to obtain a range of beam currents and corresponding propellant utilization efficiencies.

In Fig. 5(a), the ratio of the total neutral flow through the cathode is 19 percent. Enclosed keeper data exhibits higher discharge chamber losses than the SERT II open keeper data at the lower propellant utilization efficiencies but generally overlays the open keeper data at the higher utilization efficiencies. At the 24 percent fraction of total neutral flow through the cathode, the enclosed keeper data generally exhibits lower discharge chamber losses than the corresponding open keeper performance over the range of propellant utilization efficiencies tested.

Figure 6 illustrates a further comparison of the discharge chamber losses as a function of propellant utilization efficiency between open and enclosed keeper configurations for mercury propellant. For a given thruster geometry and a constant discharge chamber voltage, thruster operation is restricted to a single curve regardless of the ab-

solute values or ratios of the propellant flow. Open keeper results are presented for discharge chamber voltages of 34 volts and 38 volts. Data from the enclosed keeper operation exhibits this same general trend for 36 and 38 volt discharges. With the enclosed keeper at constant discharge chamber voltage, the discharge chamber losses rise sharply at the higher propellant utilization efficiencies.

In general, mercury results have shown that thruster performance with an enclosed keeper is comparable to that of the open keeper design. As another observation discharge chamber voltages apparently exhibit a wider range for enclosed keeper operation.

#### Argon Performance

High and low keeper power limits. - The performance data from initial tests with argon has outlined two limits to the discharge chamber operation. These limits are characterized by the keeper power level. Figure 7 summarizes these preliminary results and illustrates the low and high keeper power levels. In this figure the discharge chamber losses are shown as a function of propellant utilization efficiency for constant neutral flow to the thruster. The high keeper power limit (~30 watts) was characterized by keeper discharge currents between 1 and 1.5 amperes and keeper voltages between 20 and 30 volts (the lower boundary of the shaded area). The lower limit (~5 watts) was characterized by a current around 0.3 amperes and voltages between 15 and 18 volts (the upper boundary of the shaded area). These keeper power levels may be compared to the SERT II (mercury) keeper power of 3.3 watts, 0.3 amperes at 11 volts. Because the ionization potential of argon is 15.76 volts, higher keeper voltages would be expected in addition to higher discharge voltages than during mercury (10.2 volt ionization potential) operation.

Outside the shaded keeper power limits, shown in Fig. 7, the keeper or chamber discharge became unstable and could not be maintained. If the thruster was operating at point A (fig. 7) at the high keeper power limit and the keeper current was reduced ( $J_1$  remaining constant), the beam current decreased. This decreased in beam current lowered the propellant utilization efficiency and increased the eV/ion as illustrated by point A'. At point A', if the keeper discharge current was lowered further, the current would drop to zero extinguishing the discharge. The magnitude of this lower power limit varied for different neutral total flow rates and ratios of cathode to total flow. In general, once the keeper current was less than 0.5 amperes, the keeper discharge became unstable.

At the high power limit, if the keeper discharge current was increased, the main discharge became unstable with oscillations in both the discharge chamber voltage ( $\Delta V_1$ ) and the emission current ( $J_1$ ). At these conditions, the large keeper discharge current was reducing the electron current available to the main discharge. The discharge chamber voltage would rise to attempt to draw the discharge current. These voltage excursions would lead to cathode emission currents as high as 8 amperes. In many cases, once the discharge chamber voltage began to rise, the main discharge would simply extinguish. Operating at a

higher emission current, as illustrated by point B in Fig. 7, produced the same type of keeper discharge limited operation.

The high keeper power levels were very damaging to the front surface of the cathode. Ion bombardment of the front cathode surface caused severe sputtering erosion and overheating of the cathode. In the process of understanding and defining the limits of allowable keeper operation, the cathode used in the mercury calibration runs was destroyed. Multiple startings were very hard on the cathode because the initiation and stabilization of the discharge required keeper currents of two amperes for a few minutes. Subsequent operational experience has reduced both the number of times the cathode must be restarted and the starting keeper current to 1 ampere and below. Design of the cathode and keeper electrodes for the range of discharge and keeper currents necessary for a particular application should provide acceptable cathode lifetimes.

Discharge chamber operating characteristics. - Figure 8 illustrates the discharge chamber performance for argon at the high and low keeper power levels. All the argon results are for an enclosed keeper with a 3.2 mm diameter aperture and spaced 0.76 mm from the cathode tip. The results in Fig. 8 are for a hollow cathode with a 0.76 mm diameter orifice. As previously mentioned, the cathode used in the mercury calibration runs (0.38 mm diameter orifice) was ruined during the initial gas operations. The net accelerating voltage,  $V_1$ , and the accelerator voltage,  $V_A$ , were 3000 and -2000 volts respectively throughout these tests unless otherwise noted. The divergent magnetic field was maintained at the same value as used in the mercury calibration runs ( $4 \times 10^{-3}$  W/m<sup>2</sup> on axis at the baffle position). The neutral flow rate was held constant at 0.64 amperes with 39 percent of the total flow through the cathode.

At the high keeper power limit of approximately 30 watts, the discharge chamber losses were 175 eV/ion for propellant utilization efficiencies up to 63 percent. At this point the discharge chamber losses increased rapidly to approximately 300 eV/ion at a maximum utilization efficiency of 70 percent. For this high power limit, the discharge chamber voltage increased from 63 volts at 40 percent utilization up to 80 volts at 70 percent utilization. Propellant utilization efficiencies beyond 70 percent were not attainable in the high power limit because of the high discharge voltage (100 V) and subsequently unstable operation.

In the low keeper power limit of approximately 4 watts, the discharge chamber losses vary from 260 eV/ion at 60 percent utilization to 335 eV/ion at 84 percent utilization. At utilization efficiencies beyond 84 percent the keeper discharge could not be maintained.

These results demonstrate that the discharge chamber losses as a function of propellant utilization efficiency were essentially independent of the keeper power level. However, the advantage of operating at the lower keeper power limits were lower discharge chamber voltage and reduction in cathode degradation due to ion bombardment.

Propellant utilization efficiency and dis-

charge chamber losses were calculated assuming single ionization ( $Ar^+$ ). Over the range of discharge chamber voltages (50 to 80 V) obtained for the argon performance data, this may not be strictly correct. The cross section for multiple ionization of argon becomes appreciable (greater than 10 percent) for primary electron energies greater than 80 volts.<sup>(8)</sup> However, these energies are, in general, for neutral atoms in the ground state. The presence of excited neutral and ions will increase the effective cross section for multiple ionization. On the other hand, the plasma potential inside the distributor pole piece is of the order of the keeper voltage.<sup>(9)</sup> This potential should be subtracted from the discharge chamber voltage to give a modified discharge voltage on the order of 50 volts. The plasma potential drop within the keeper region may lower the effective electron energy available for multiple ionization. Although the effect of multiple ionization was not included in this preliminary investigation, the examination of the effect should be included in future experiments if a monoenergetic beam is desired.

Figure 9 shows the discharge chamber characteristics for a higher fraction of the total neutral flow through the cathode. For a total neutral flow of 0.684 amperes, with 52 percent of the flow through the cathode, the curves of the discharge chamber losses as a function of propellant utilization efficiency outlining the limits of high and low keeper power levels lie relatively close together. Incorporating the keeper discharge power into the eV/ion calculations for both the high and low keeper power levels is also represented on the figure. Propellant utilization efficiencies greater than 70 percent was attainable for each power level. Examination of the discharge chamber voltage as a function of propellant utilization efficiency shows no difference between high and low keeper power levels in addition to a relatively constant discharge voltage of 61 to 63 volts.

Figure 10 illustrates the discharge chamber characteristics as a function of propellant utilization efficiency for various combinations of cathode and main propellant neutral flow. Results are presented for a typical neutral flow rate of 0.75 amperes. The cathode used for this particular test had a large chamfer as a result of extended operation in another mercury thruster. The orifice had a minimum diameter of 0.3 mm and a maximum diameter of 1.6 mm.

In general, the range between the high and low keeper power limits was very narrow for this particular series of runs, so that only one set of data was taken between these limits. The typical keeper power was about 14 watts. Maintaining the discharge at lower keeper power levels was not possible because of keeper discharge instability. Operating at higher keeper power levels led to a serious degradation of thruster performance as well as unstable discharge characteristics. Data in Figs. 10(a) through 10(d) are presented for the minimum keeper level available to maintain stable operation.

Figure 10(a) presents the results for a cathode flow rate of 87.6 percent of the total neutral flow. The result of including the keeper power into the eV/ion calculation is also plotted on the curves representing the discharge chamber losses.

The data presented in Fig. 10(a) represent the lowest discharge chamber losses for argon over this wide range of propellant utilization efficiencies obtainable to date. In addition, the discharge chamber voltage as a function of propellant utilization efficiency is the lowest of the series of runs (10(a) - 10(d)).

As the fraction of neutral flow through the cathodes was reduced to 74.5 (fig. 10(b)) and 48.5 percent (fig. 10(c)) of the total neutral flow respectively, both the discharge chamber losses and the discharge voltage as a function of propellant utilization efficiency increased above those results obtained with a high cathode flow fraction (fig. 10(a)).

The minimum cathode flow rate necessary to maintain stable cathode operation was approximately 0.25 amperes of neutral flow. Results of thruster operation at this low cathode flow limit are presented in Fig. 10(d). The cathode flow comprised 33 percent of the total flow for these results. Although the discharge chamber losses were between 360 and 400 eV/ion, the discharge voltage was relatively high at 72 volts. This high discharge voltage may have contributed to double ionization ( $\text{Ar}^{++}$ ) which probably explains propellant utilization efficiency measurements above 90 percent.

The preceding argon performance results have been presented for a net accelerating potential,  $V_1$ , of 3000 volts and an accelerator potential,  $V_A$ , of -2000 volts. Figure 11 presents the discharge chamber losses as a function of propellant utilization efficiency for two different net accelerating potentials. The keeper power is included in the eV/ion calculation. The ratio  $R$ , between the net accelerating voltage,  $V_1$ , and the total accelerating voltage,  $V_1 + |V_A|$ , was held constant at a value of 0.6. Cathode flow rate was 87.5 percent of the total neutral flow of 0.761 amperes (see fig. 10(a)). Results show an approximate 40 eV/ion increase in the discharge chamber losses for a decrease of 1000 volts in the net accelerating potential. This trend is generally consistent with mercury thruster operation.

#### Comparison With Previous Results

It is possible to make a general comparison between thruster performance using argon and mercury propellants for enclosed keeper operation. For argon operation, the keeper power level played a major role in maintaining discharge stability. Mercury results, on the other hand, were relatively insensitive to the keeper power levels. The discharge chamber voltage,  $\Delta V_1$ , was higher for argon. This follows directly from the fact that the ionization potential of argon is about 50 percent higher (15.76 volts compared to 10.2 volts) than mercury. The ratio of the range of discharge chamber voltages for mercury (33 to 45 V, see fig. 2(b)) to the range of discharge chamber voltages for argon (52 to 70 V, see fig. 10) is equal to the ratio of the ionization potentials of argon to mercury. With argon, a wider range of cathode flow rates ( $J_{ok}/J_o = 0.33$  to 0.875) was possible while maintaining reasonable discharge chamber performance (eV/ion) and encompassing a wide range of propellant utilization efficiencies. With mercury, reasonable performance was obtained within a rather limited range of cathode flow rates

( $J_{ok}/J_o = 0.19$  to 0.30). These results indicate that with the argon propellant far larger keeper power was required for stable operation than with mercury propellant.

Figure 12 compares the discharge chamber losses as a function of propellant utilization efficiency for two bombardment thrusters using mercury and argon. The 1964 performance data(1) obtained with a 10-cm thruster and a thermionic (wire) cathode had relatively low propellant utilization efficiency and high discharge chamber losses. Advances in thruster component technology since this time have resulted in substantial improvements in both decreased discharge chamber losses and increased propellant utilization efficiency. The performance of the SERT II discharge chamber using mercury is representative of the present level of technology. The present results with argon are equally impressive. These advances in thruster component technology have made possible not only an increase in argon propellant utilization efficiency to values above 85 percent but also a reduction in the discharge chamber losses to values around 240 eV/ion.

#### Concluding Remarks

A modified SERT II type, 15-cm electron bombardment thruster has been tested with both mercury and argon propellants. Mercury performance results with an enclosed keeper were found to be generally comparable to those obtained with an open keeper (SERT II). The enclosed keeper did permit a wider range of discharge operating parameters such as cathode flow rate and discharge chamber voltage.

Preliminary argon results presented in this paper indicate that reasonably good discharge chamber performance can be obtained over a wide range of propellant utilization efficiencies. The discharge was strongly effected by the cathode keeper discharge power level. Design of the cathode and keeper electrodes for the emission currents necessary for a particular application will provide acceptable lifetimes.

A long life, high efficiency electron-bombardment ion source operating on a variety of propellants should find application in a variety of potential areas. Some of these areas include discharge chamber diagnostics, preflight component and system checkout, ion plating, implantation and machining, as well as a general plasma source.

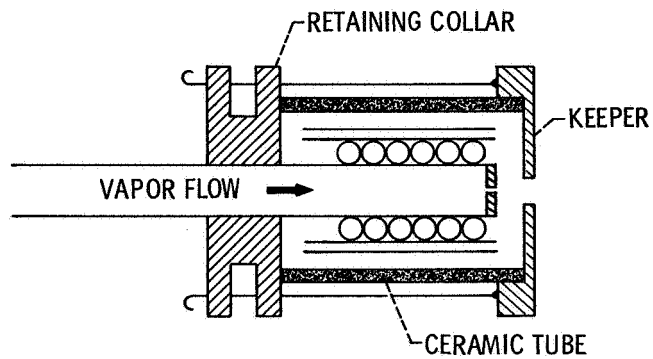
#### Symbols

$E_1$	discharge chamber losses, eV/ion
$J_E$	cathode emission current, amps
$J_{ok}$	cathode neutral propellant flow, equivalent amps
$J_{om}$	main neutral propellant flow, equivalent amps
$J_o$	total neutral propellant flow, equivalent amps
$P_1$	pressure downstream of piston, torr

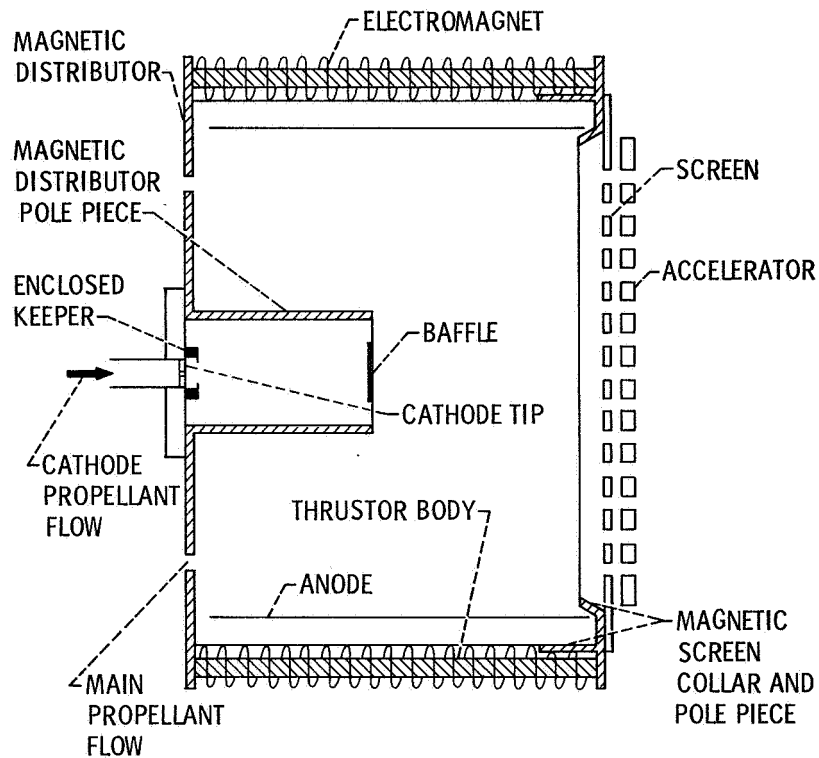
R	ratio of net accelerating voltage to total accelerating voltage, $V_1/(V_1 +  V_A )$
$R_0$	gas constant
$T_1$	temperature downstream of piston, $^{\circ}\text{K}$
$V_A$	accelerator voltage, volts
$V_D$	volume displacements, liters
$V_1$	net acceleration voltage, volts
$\eta_u$	propellant utilization efficiency, percent
$\Delta t$	time lapse for displacement, sec
$\Delta V_1$	ion discharge chamber voltage, volts
$\rho_1$	gas density downstream of piston, $\text{kg/m}^3$

#### References

1. Reader, P. D., "The Operation of an Electron-Bombardment Ion Source with Various Gases," presented at the International Conference on Electron and Ion Beam Science and Technology, Electrochemical Society and ASME, Toronto, Canada, May 5-7, 1964.
2. Kerslake, W. R., Byers, D. C., and Staggs, J. F., "SERT II Experimental Thruster System," Paper No. 67-700, Sept. 1967, AIAA, New York, N.Y.
3. Byers, D. C. and Staggs, J. F., "SERT II: Thruster System Ground Testing Performance," Journal of Spacecraft and Rockets, Vol. 7, No. 1, Jan. 1970, pp. 7-14.
4. Reader, P. D., Nakanishi, S., Lathem, W. C., and Banks, B. A., "A Sub-Millipound Mercury Electron-Bombardment Thruster," Paper No. 70-616, June 1970, AIAA, New York, N.Y.
5. Bechtel, R. T., Csiky, G. A., and Byers, D. C., "Performance of a 15 Centimeter Diameter Hollow Cathode Kaufman Thruster," Paper No. 68-88, Jan. 1968, AIAA, New York, N.Y.
6. Keller, T. A. and Wise, G. A., "Experimental Results of a 1500-Cubic-Foot Unbaked Ultra High Vacuum System," High Vacuum Technology Testing and Measurement Meeting, TM X-1268, 1966, NASA, Cleveland, Ohio, p. 19-25.
7. Ferguson, H. and Sovey, J. S., "Performance Tests of a 1/2-Millipound (2.2 mN) Ammonia Resistojet Thruster System," TN D-4249, 1967, NASA, Cleveland, Ohio.
8. Kieffer, L. J. and Dunn, G. H., "Electron Impact Ionization Cross-Section Data for Atoms, Atomic Ions, and Diatomic Molecules: I. Experimental Data. Reviews of Modern Physics, Vol. 38, No. 1, Jan. 1966, pp. 1-35.
9. Bechtel, R. T., "Component Testing of a 30-Centimeter Diameter Electron Bombardment Thruster," Paper No. 70-1100, Aug. 1970, AIAA, New York, N.Y.



(a) Sketch of enclosed keeper cathode



(b) Thruster

Figure 1. - Sketch of 15-cm. diameter electron bombardment thruster.



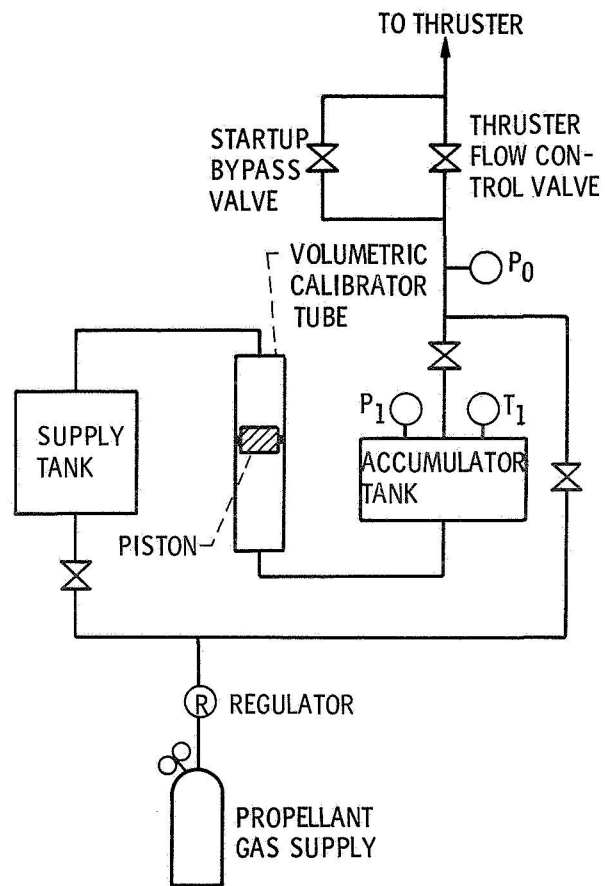


Figure 2. - General schematic of cathode mass flow calibration system.

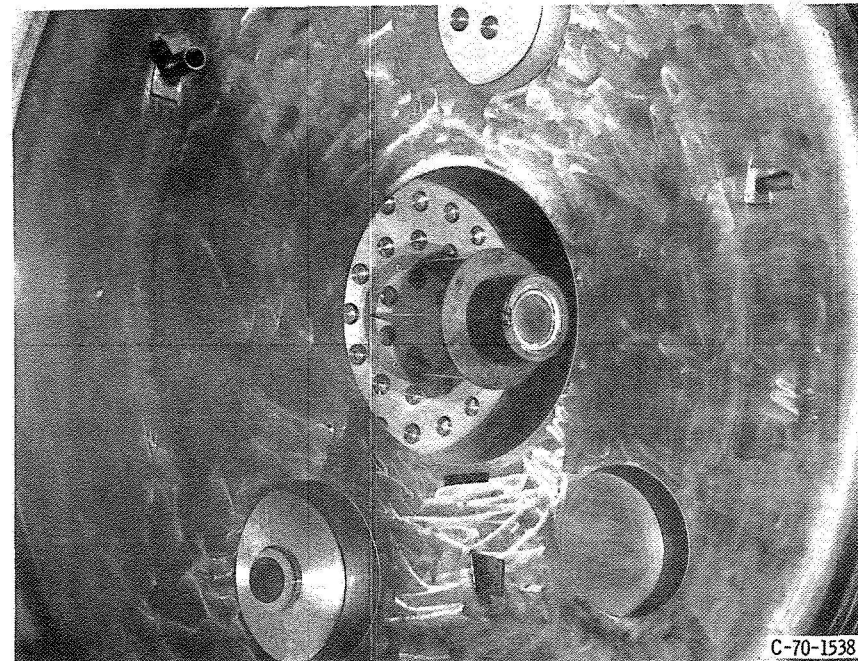


Figure 3. - 15 cm thruster mounted in the vacuum facility used for argon propellant operation.

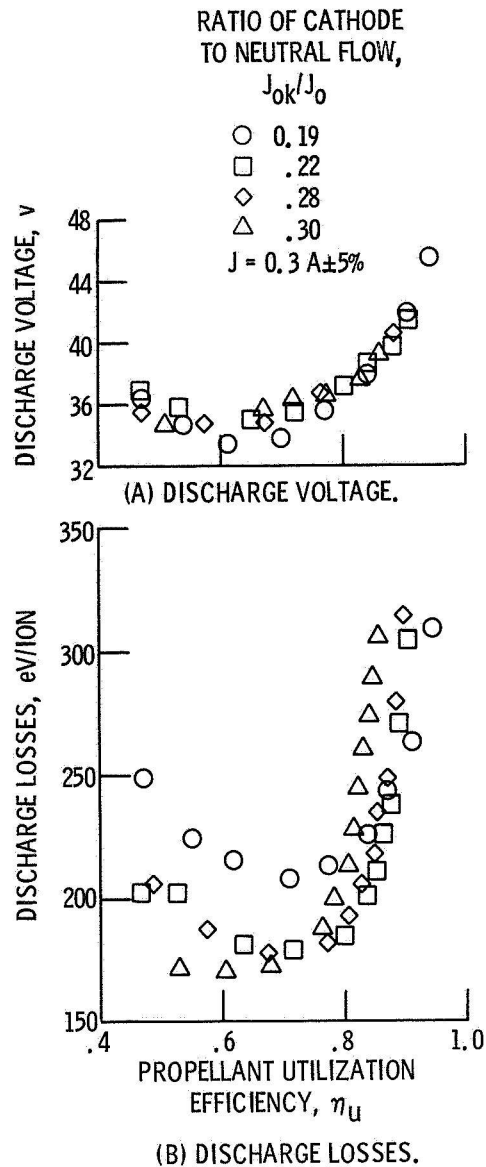


Figure 4. - Discharge chamber performance with an enclosed keeper cathode with mercury for various combinations of cathode and main propellant flow. Cathode aperture was 0.4 mm diameter.

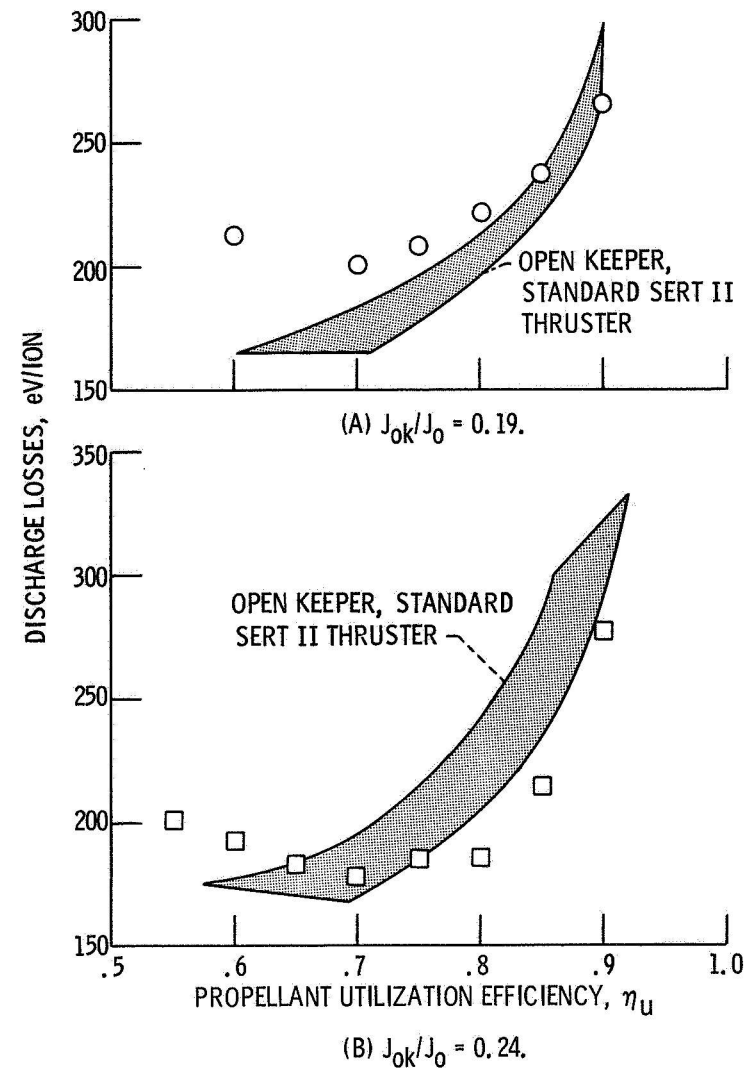


Figure 5. - Comparison of the discharge chamber losses between open and enclosed keeper cathodes for mercury for two different combinations of cathode and main propellant flow. Neutral flow was typically 0.3 amperes.

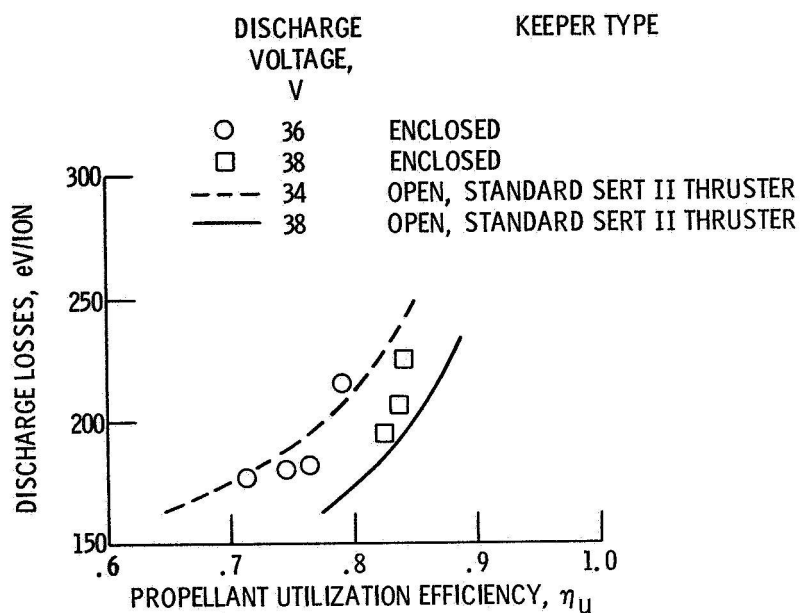


Figure 6. - Comparison of the discharge chamber performance between open and enclosed keeper cathodes with mercury at constant discharge voltage.

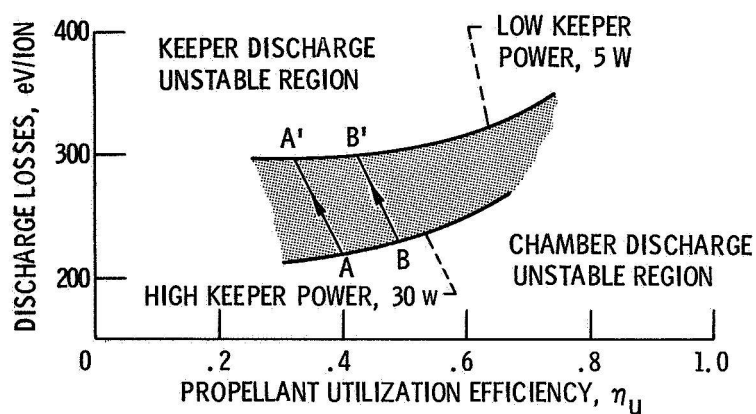


Figure 7. - Typical discharge chamber characteristics for argon illustrating high and low keeper discharge power limits for constant neutral flow.

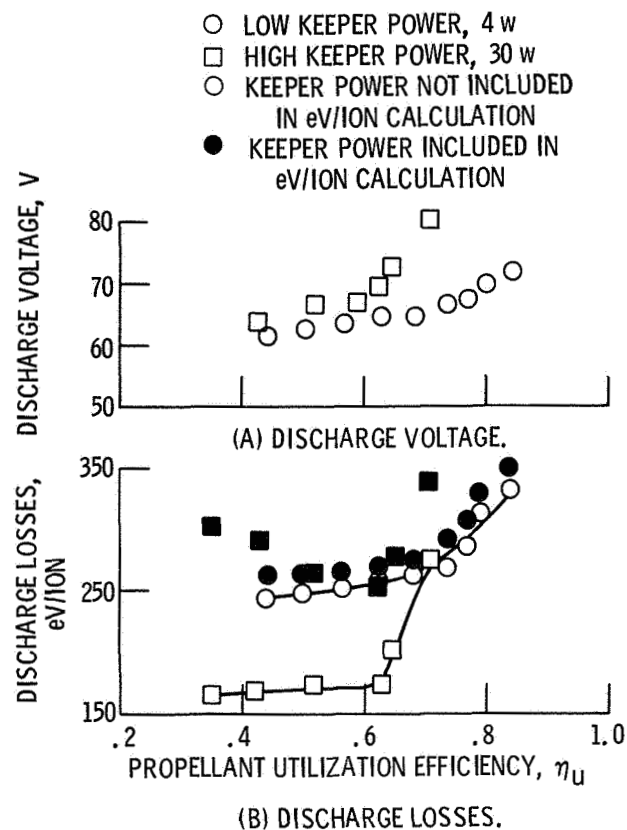


Figure 8. - Discharge chamber performance with an enclosed keeper cathode with argon at the high and low keeper power levels;  $J_0 = 0.64$  amperes,  $J_{ok}/J_0 = 0.39$ ,  $V_I = 3000$  V,  $V_A = -2000$  V, cathode orature was 0.76 mm diameter.

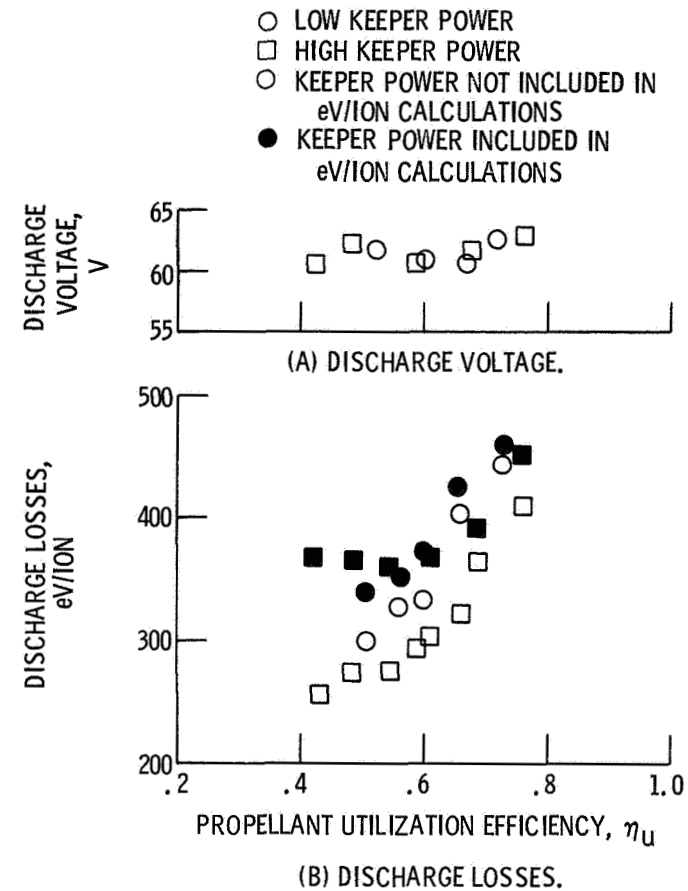


Figure 9. - Discharge chamber performance with argon for  $J_0 = 0.68$  amperes,  $J_{ok}/J_0 = 0.52$ , cathode aperture was 0.76 mm diameter.

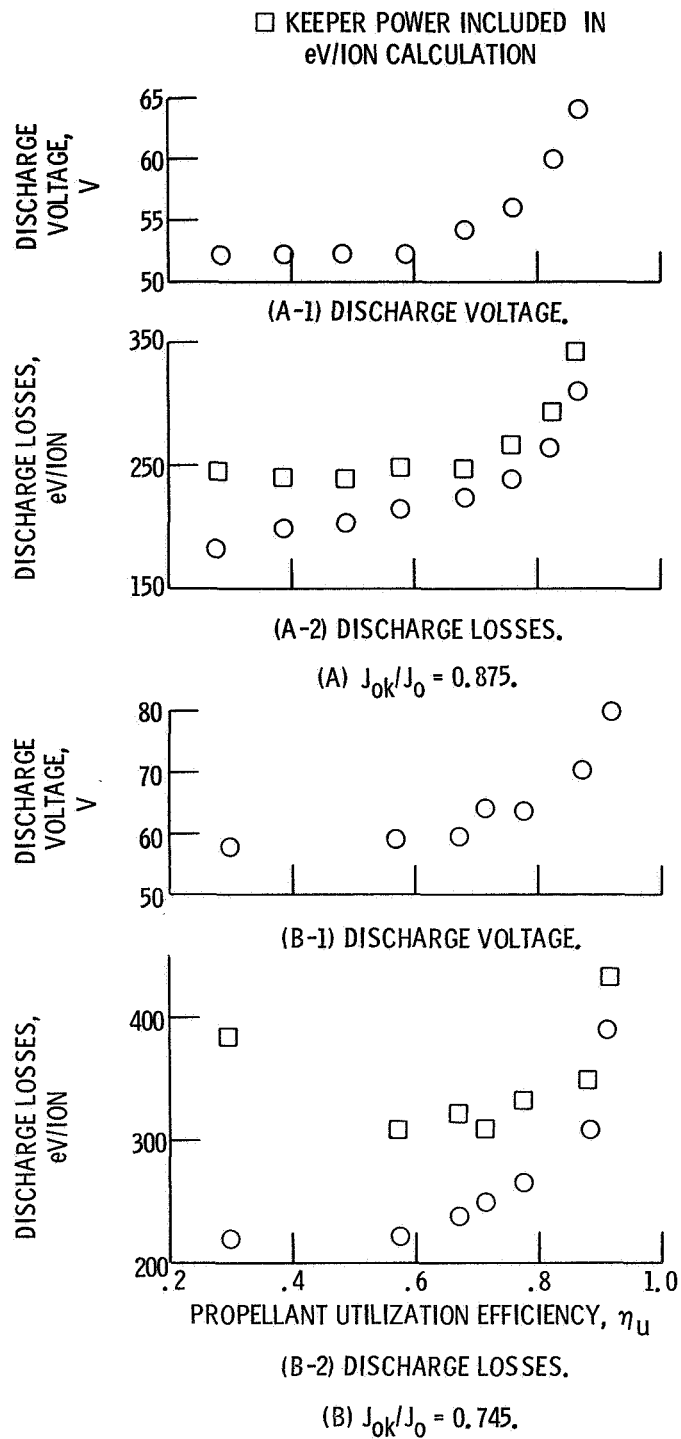


Figure 10. - Discharge chamber performance with argon for various combinations of cathode and main propellant flow,  $J_0 = 0.75$  A  $\pm 2$  percent, cathode aperture was 0.3 mm diameter.

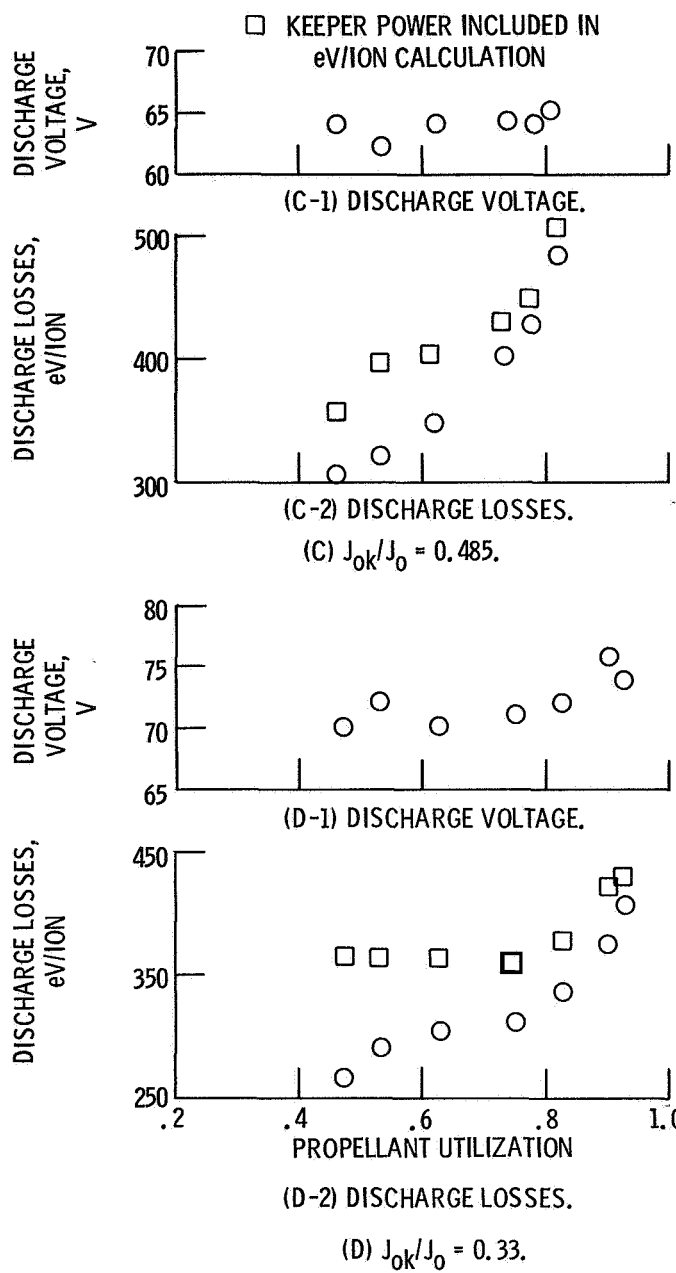


Figure 10. - Concluded.

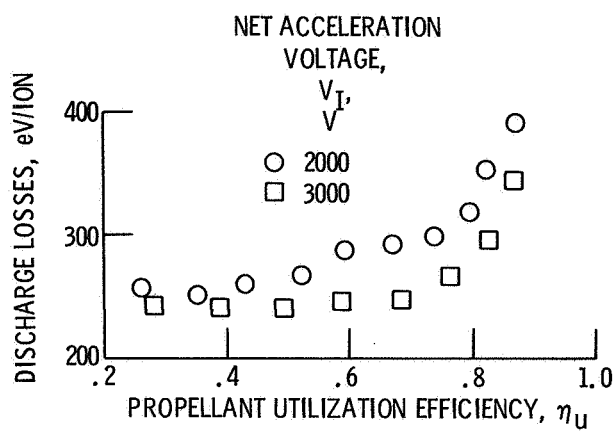


Figure 11. - Discharge chamber performance with argon for two different accelerator voltages,  $R = V_I / (V_I + |V_A|) = 0.6$ ,  $J_0 = 0.76$  amperes,  $J_{0k}/J_0 = 0.875$ , cathode aperture was 0.76 mm diameter.

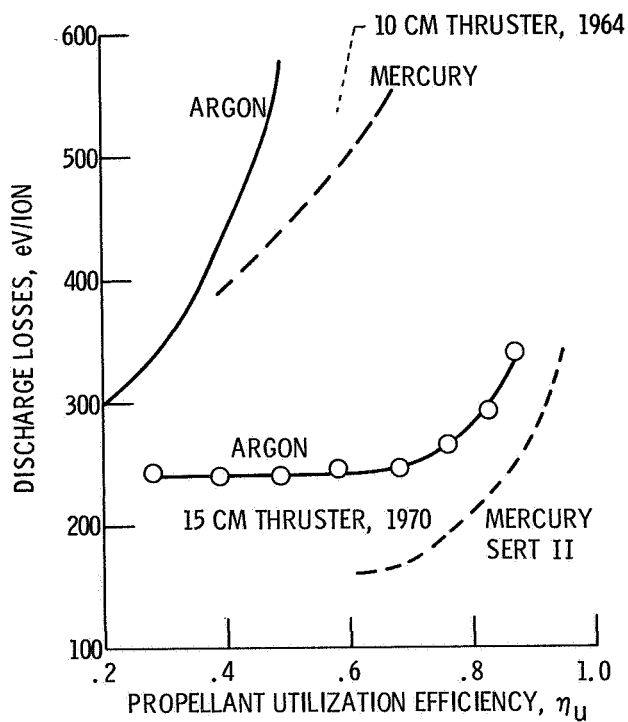


Figure 12. - Comparison of the discharge chamber performance for two bombardment thrusters using mercury and argon propellant.